Available online at www.sciencedirect.com

ScienceDirect

Procedia CIRP 55 (2016) 89 – 94

www.elsevier.com/locate/procedia

5th CIRP Global Web Conference Research and Innovation for Future Production

The Scanning Dimensional Microelectrochemical Machining with the Ultra-Small Interelectrode Gap

Victor Lyubimov[1,*], Vladimir Volgin[1], Inna Gnidina[1] and Vladislav Krasilnikov[1]

[1]*Tula State University, pr. Lenina 92, Tula 300012, Russia*

* Corresponding author. Tel.: +7-4872-35-26-81; fax: +7-4872-35-26-81. E-mail address: lvv@tsu.tula.ru

Abstract

The process of the micro electrochemical machining with the ultra small interelectrode gap without the electrode-tool displacement for the flushing with the workpiece scanning by the electrode-tool and with F_{et}/F_{wp} = 0.5 – 25 % is considered in the publication. The modeling of the MECM process at the various electrode-tool paths on X- and Y-axes with periodic updating of the UIEG on Z-axis during the anode dissolution of the workpiece is executed.

Peer-review under responsibility of the scientific committee of the 5th CIRP Global Web Conference Research and Innovation for Future Production

Keywords: Interelectrode Gap; Anode Dissolution; Electrode-Tool; Scanning Microlectrochemical Machining

1. Introduction

The dimensional microelectrochemical machining (μECM) is a highly efficient method of fabrication of complex geometries in difficult to machine materials [1, 2].

Error processing with the use of μECM depends substantially on the magnitude of the interelectrode gap (IEG) S in accordance with Δ=k*S, where k is the coefficient of proportionality. [3].

In recent years, good results were obtained when ultra-small IEG on the order of 5-10 μm were applied in the case of copying diagrams, i.e. when $F_{ET}=F_{wp}$, where F_{ET} is the electrode-tool (ET) surface area, F_{wp} is the treatment surface area [5]. However, a significant decrease in the interelectrode space when applying the ultra-small IEG requires periodic flushing from products of electrode reactions. Therefore, loop mode and pulse-loop mode of the μECM (Fig. 1) were developed [1, 4].

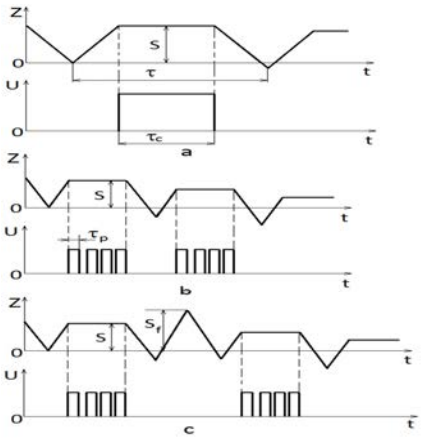

Fig.1. Diagrams of dimensional electrochemical machining: (a) loop mode; (b) pulse-loop mode; (c) pulse-loop mode with a ET tap to the IEG flushing; S_f – flushing IEG ; τ_p – pulse width; τ_c , τ – work-loop width and the total-loop width; U – applying voltage; the z coordinate of the electrode tool displacement.

Peer-review under responsibility of the scientific committee of the 5th CIRP Global Web Conference Research and Innovation for Future Production
doi:10.1016/j.procir.2016.08.032

It follows from the diagrams above that the ratio τ_c/τ declines at the transition to the ultra-small IEG. The result is that the average removal velocity of the workpiece material is substantially less than the initial velocity of anodic dissolution in the loop (Fig. 2).

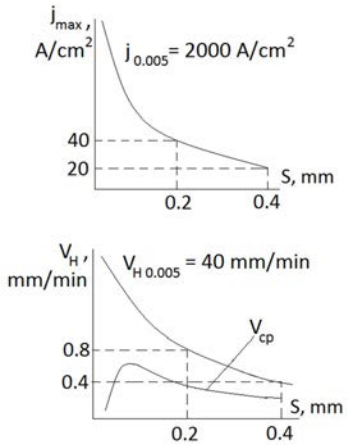

Fig. 2 . The change of technological parameters depending on the IEG: V_H – the nominal calculated velocity of the anodic dissolution; j – the anode current density.

Thus, a significant IEG reduction (8-80 times) providing increase of machining precision, does not lead to productivity increasing, and to its significant reduction. This situation necessitates the search for other save methods of initial interelectrode media properties.

One of the effective ways is the μECM at ultra-small end IEG with the applying of unshaped or partially shaped electrode tool moving along the axes Ox, Oy and periodic adjustment IEG along the axis Oz (Fig. 3) [6, 7].

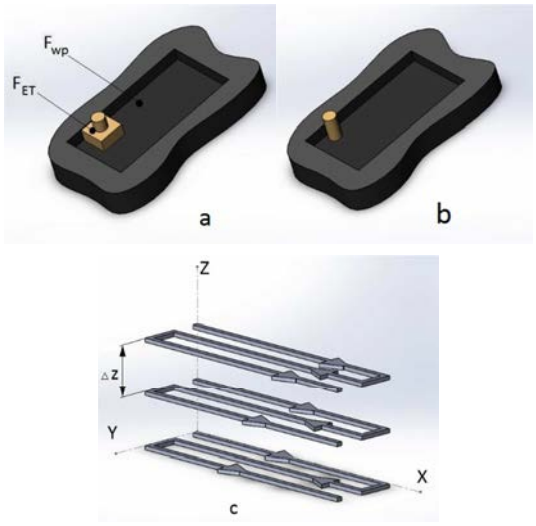

Fig. 3. The technological scheme of the dimensional ECM unshaped (b) and partially shaped (a) electrode-tool; (c) the cyclogram of the electrode-tool displacement.

In this case, we can expect that the average velocity of anodic dissolution can be calculated as:

$$V_{cp} = V_H \cdot \frac{F_{ET}}{F_{WP}}. \quad (1)$$

The electrode tool displacement along a predetermined path (Fig. 4) provides the cavity geometry. The proposed technological scheme allows to produce anodic dissolution of the workpiece in a continuous mode with a loop electrode tool displacement along the axis Oz by the value of anodic dissolution ΔZ in loop.

The scanning μECM can be perform at two different relative locations of the workpiece and ET: vertical (Fig. 4a.) when the ET axis is perpendicular to the workpiece surface and the horizontal (Fig. 4b.) when the ET axis is parallel to the workpiece surface.

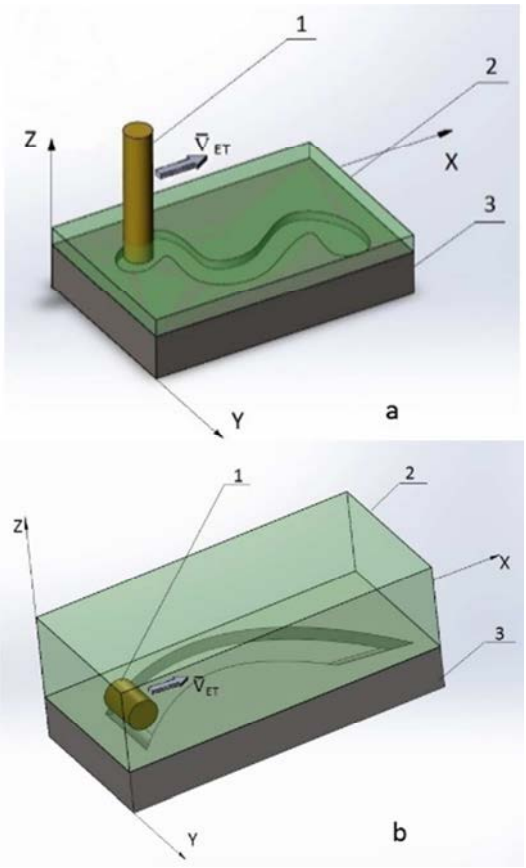

Fig. 4. The schemes of electrochemical machining by ET displacement along a predetermined path: (a) μECM with vertical ET; (b) μECM with horizontal ET; 1 – the electrode tool, 2 – electrolyte, 3 – workpiece; $\bar{V}_{ET}$ – ET displacement velocity.

The aim of this work is a theoretical study of scanning electrochemical machining for establishment of regularities (dependencies) of technological parameters with the process conditions.

2. The statement of the problem and basic equations

A constant electrolyte renewal is required to reduce the influence of electrochemical reactions products on the anodic dissolution velocity of the workpiece along the entire IEG length that leads to the μECM constancy as is known. The effective process of anodic dissolution is possible when volumetric gas content and temperature do not exceed the magnitudes of 0,7 and the boiling point of the electrolyte solution, respectively, as the continuity of the working fluid liquid phase is disrupted in this case. It requires the maintenance of certain flow velocity and pressure of the electrolyte in the IEG. It is desirable that the sludge removal velocity exceeded the speed of its formation, which in turn has a positive effect on the increase of machining precision. Therefore, the first step of modeling is the determination of the electrolyte pressure and the flow velocity in the IEG for different ET velocities of the magnitudes of the interelectrode gap.

The treatment scheme with the horizontal ET was used in the theoretical study of the μECM under the condition of the electrode tool displacement along the workpiece, because it makes use of a two-dimensional model of the electrochemical treatment process.

The computational domain, shown in Fig. 5 was used in the mathematical simulation. We consider that the electrode-tool is stationary, the electrolyte solution and the workpiece move at a velocity V_{ET} to simplify the modeling of transport processes. The following assumptions in the simulation were introduced: the electrolyte is a Newtonian liquid; the viscosity is constant; the slide on the border "electrode-electrolyte" is missing; the influence of the surface layer can be neglected; the electrolyte is incompressible liquid.

The Navier-Stokes equations for incompressible viscous fluid were applied to describe the electrolyte flow:

$$\begin{aligned} &\frac{\partial v}{\partial t} + v\cdot\frac{\partial v}{\partial x} + u\cdot\frac{\partial v}{\partial z} = \frac{\mu}{\rho}\cdot\left(\frac{\partial^2 v}{\partial x^2} + \frac{\partial^2 v}{\partial z^2}\right) - \frac{1}{\rho}\cdot\frac{\partial p}{\partial x} \\ &\frac{\partial u}{\partial t} + v\cdot\frac{\partial u}{\partial x} + u\cdot\frac{\partial u}{\partial z} = \frac{\mu}{\rho}\cdot\left(\frac{\partial^2 u}{\partial x^2} + \frac{\partial^2 u}{\partial z^2}\right) - \frac{1}{\rho}\cdot\frac{\partial p}{\partial z} \end{aligned} \quad (2)$$

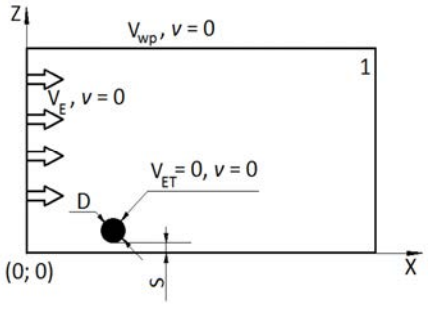

Fig. 5. The geometry of the computational domain: 1 – electrolyte; V_E is the flow velocity of the electrolyte, Vwp is the velocity of the workpiece, V_{ET} is the electrode tool velocity, D is the electrode-tool diameter, S is the interelectrode gap, v is the kinematic viscosity of the electrolyte.

We obtain the hydrodynamic velocity distribution of the electrolyte solution in the interelectrode gap on the result of the numerical solution of the equations (2). It allows to determine the average magnitude of its horizontal component:

$$V_E = \frac{1}{S}\int_0^S V dZ \ . \quad (3)$$

Gaseous products and heat evolve in the IEG during the electrochemical treatment. The interelectrode media properties change as a result. Thus electrical conductivity may be calculated by the following equation:

$$\chi = \chi_0 \cdot [1 + \beta\cdot(T - T_0)]\cdot(1-\xi)^n, \quad (4)$$

where χ_0 is the specific electric conductivity of the electrolyte at a temperature T_0; T_0 is the initial temperature of the electrolyte; ξ is the volumetric gas content; n = 1.5; β is the temperature coefficient, assumed equal to 0.015.

The magnitude of the current density is determined by the following equation [8]:

$$i_a = \frac{\chi\cdot U}{S} = \frac{\chi_0\cdot[1+\beta\cdot(T-T_0)]\cdot(1-\xi)^n U}{S} \ . (5)$$

The temperature and gas filling of the electrolyte change in length of the interelectrode gap and depend on the flow velocity of the solution in the interelectrode gap. The following equation can be used to determine their values [8]:

$$\xi = \xi_0 + \frac{K_H\cdot i_a\cdot D}{\rho_H\cdot V_E\cdot S}, \quad (6)$$

$$T = T_0 + \frac{U\cdot i_a\cdot D}{c_E\cdot\rho_E\cdot V_E\cdot S}, \quad (7)$$

where K_H is the electrochemical equivalent of hydrogen; S is the magnitude of the interelectrode gap, m; χ is the specific electric conductivity of the electrolyte; c_E is the specific heat of electrolyte; ρ_E is the density of the electrolyte.

The density of hydrogen ρH is based on:

$$\rho_H = \frac{\mu\cdot p_E}{R\cdot T}, \quad (8)$$

where R is the universal gas constant; μ is the molar mass of hydrogen; p_E – pressure in the IEG.

It should be noted that the magnitude ξ can take values from 0 to 1, where 0 corresponds to the liquid phase of the electrolyte, and 1 is gaseous phase.

The temperature can take values exceeding the boiling point under certain parameter values that leads to a transition of the electrolyte from the liquid phase to the gas for which the above system of equations will have a different

representation. Therefore, this system must be supplemented by the following condition:

$$T \le T_C,$$

where T_C is the boiling point of the electrolyte.

Thus, we need to solve the system of equations (4) – (8) for finding the dependence of the electrolyte temperature during the treatment on the electrode tool velocity.

3. Results and discussion.

The source data given in table 1 were used at the simulation of the flow solution in the interelectrode space were carried out.

The distribution of the flow solution velocity (Fig. 6), the dependence of the flow electrolyte velocity (Fig. 7) and pressure (Fig. 8) to the extraction plant from the displacement velocity of the electrode tool were obtained as a result of solving the Navier-Stokes equations.

Table 1. The source data for modeling

Parameters	Magnitude range
ET diameter, μm	250
IEG, μm	5 – 75
ET velocity, m/s	0,25 – 32
Electrolyte	10% HF
Electrolyte dynamic viscosity, Pa*s	0,0053

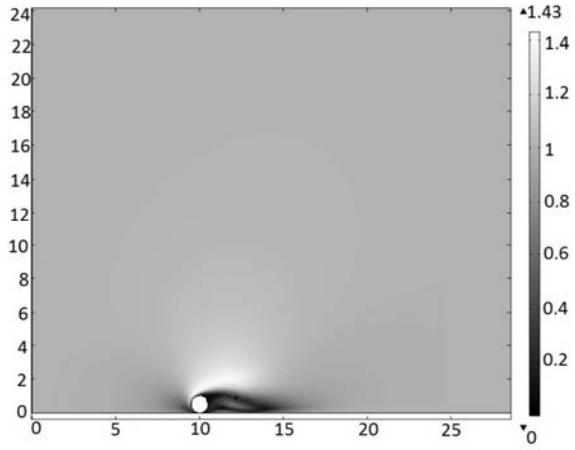

Fig. 6. The distribution of the electrolyte relative velocity (V/V_{ET}) in the interelectrode gap.

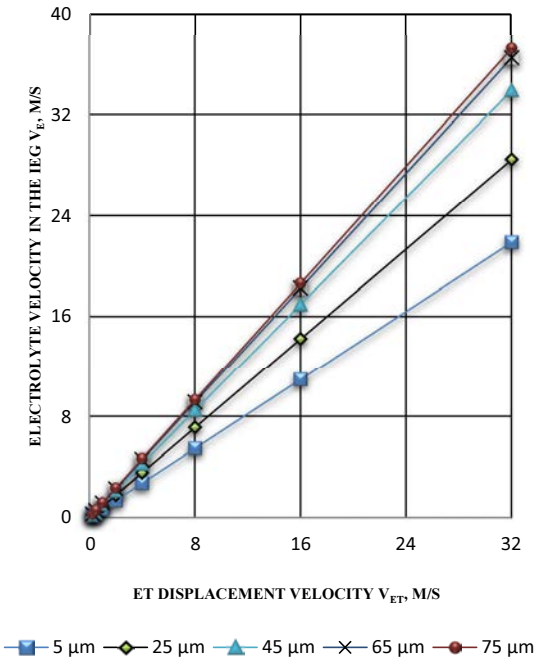

Fig. 7. The dependences of the flow electrolyte velocity in the extraction plant from the ET velocity at different interelectrode gaps.

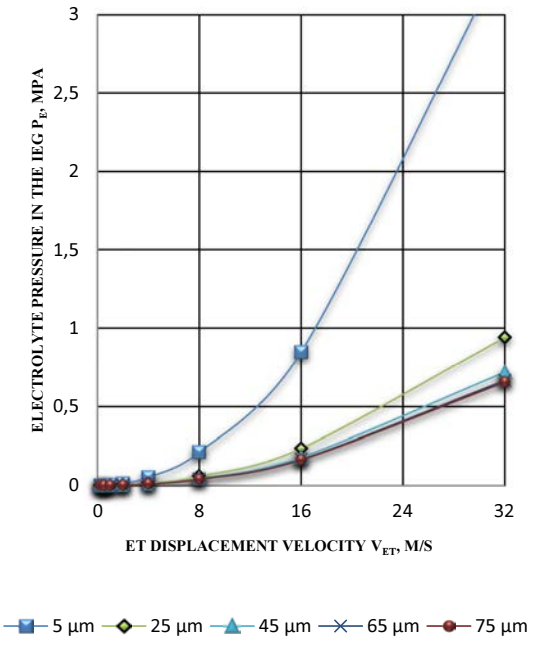

Fig. 8. The dependences of pressure in the IEG from the ET velocity at different interelectrode gaps.

The electrolyte velocity and pressure increase from 0.2 m/s to 22 m/s and from 207 Pa to 3 MPa, respectively, when the displacement velocity of the IEG changes from 0.25 m/s to 32 m/s and the magnitude of the interelectrode gap is 5 μm as follows from the obtained results. It was also revealed that the reduction of IEG magnitude leads to a decrease of the flow electrolyte velocity by 1,7 times and increasing the pressure by 5,2 times that leads to the decrease of anodic dissolution velocity of treatment material.

The dependences of V (V_{ET}) and P (V_{ET}) were used in the calculation of the gas filling and the temperature of the electrolyte. The volume fraction dependences of the gas content ξ from the displacement velocity of the electrode tool V_{ET} is shown in figure 9.

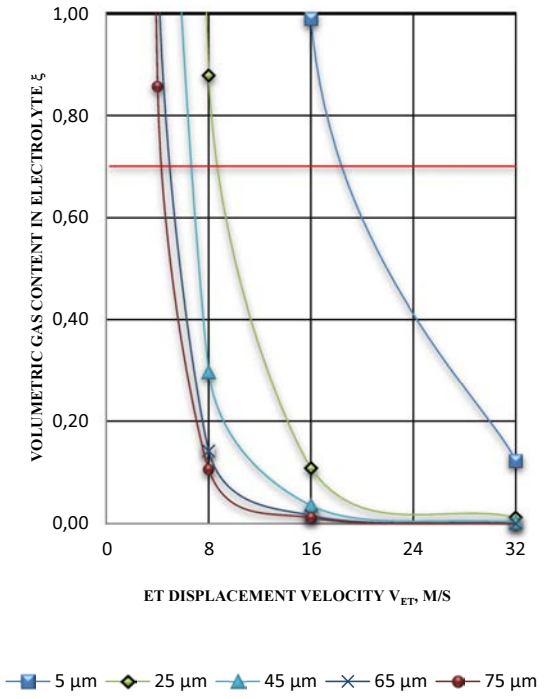

Fig. 9. The dependences of volumetric gas content from the displacement velocity of the electrode tool at different interelectrode gaps.

It was found that the minimum displacement velocity of the electrode tool is for each interelectrode gap, above which electrolyte volumetric gas content is below the critical value, equal to 0,7 as a result of calculations. For example, when the interelectrode gap is 35 μm minimum displacement velocity of the ET should be 7,4 m/s.

The next step is a study of the ET velocity influence on heating the electrolyte in the interelectrode gap (Fig. 10).

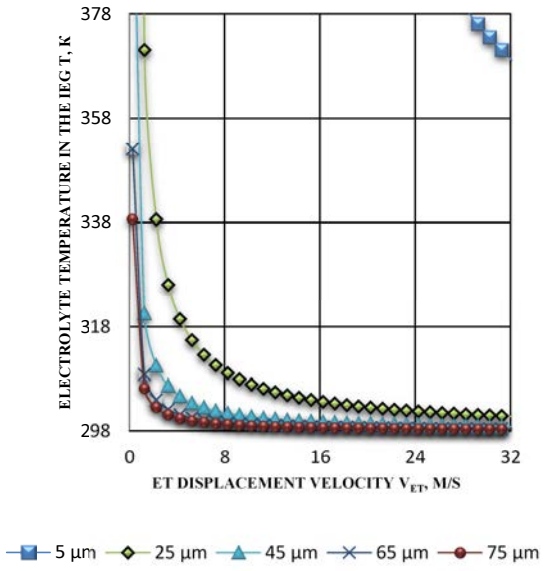

Fig. 10. The dependences of the electrolyte temperature from the displacement velocity of the electrode tool at different interelectrode gaps.

The increasing of the ET velocity from 0.25 to 32 m/s leads to a decrease of the temperature in the interelectrode gap to 298 K that provide the preservation of initial electrolyte properties in the IEG.

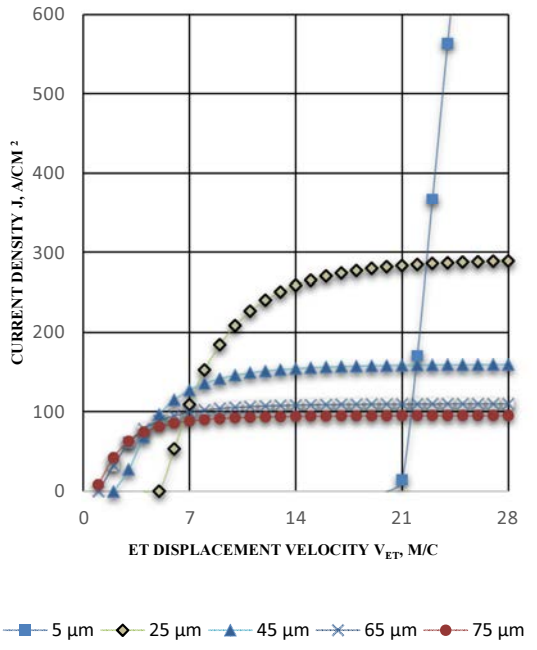

Fig. 11. The dependence of the current density from the displacement velocity of the electrode tool at different interelectrode gaps.

The dependences, shown in figure 11 and calculated from equation (4), of the current density on the ET velocity during different IEG do not originate from the center point of coordinates (0; 0) but from point ($V_{ET}^{\min}$; 0), where $V_{ET}^{\min}$ is the minimum magnitude of the ET velocity, which provides the conditions for the evacuation of products, namely constraints on the gas content and temperature, described in the second part of this publication. Thus, the minimum displacement velocity of the ET is determined by the condition of attaining the limiting magnitude of the electrolyte gas content at the IEG outlet:

$$V_{ET} \geq \frac{K_g \cdot (U - \Delta u) \cdot \chi \cdot D}{S^2 \cdot \xi_c},$$

where ξ_c is the limiting magnitude of gas content in the electrolyte.

It follows from the graph shown in figure 11 that the current density is constant after reaching a certain displacement velocity of the ET. Consequently $V_{ET}^{\max}$ is maximum velocity of the ET, the excess of which is not rational in virtue of the fact that the evacuation velocity of electrochemical reactions products is maximum at this magnitude.

Therefore, further increase of displacement velocity of the ET does not increase the current density and, as a consequence of this, the treatment productivity.

Thus, the dependences j (V_{ET}) can be divided into three regions. The first $[0; V_{ET}^{\min})$ is the region of non-stationary flow ECM process, the conditions for the evacuation of the products is not performed $\xi > \xi_c$, $T \geq T_c$. The second $[V_{ET}^{\min}; V_{ET}^{\max}]$ is the region of the rational displacement velocity of the ET, the conditions for evacuation of the products is performed $\xi \leq \xi_c$, $T < T_c$, the velocity increase leads to the increase of the process productivity. The third $(V_{ET}^{\max}; \infty)$ is the area where the velocity increase does not lead to the current density increase and process $V_{ET}^{\min} = 4\,\text{m/s}, V_{ET}^{\max} = 23\,\text{m/s}$ productivity. For example, when the IEG magnitude is 75 μm. Table 2 shows the range of rational speeds of movement of the electrode-tool for each value of the inter-electrode gap.

Table 2. Rational displacement velocity of the electrode tool at different magnitude of the interelectrode gaps.

IEG, μm	ET velocity, m/s
75	0,5-11
65	1-12
45	2-15
25	4-23
5	20-62

It should also be noted that the increase of the ET velocity is necessary at the IEG transition from 75 μm to 25 μm, because the formation velocity of the electrochemical reaction products will increase and products evacuation will decline due to the decrease of the interelectrode space in this case.

4. Conclusions

The paper presents a theoretical study of scanning electrochemical treatment. The influence of the ET velocity on the magnitude of gas content and temperature in the IEG, to preserve the initial parameters of the working fluid was investigated, and the rational values of the ET velocity were determined.

It follows from the research that anodic dissolution velocity cannot be calculated by the equation (1) at the real conditions, because the temperature of the electrolyte and the gas filling in the IEG strongly influence on the anodic dissolution process. Therefore, the coefficient k_1 must be enter into this equation, which takes into account this effect:

$$V_{cp} = k_1 \cdot V_{н} \cdot \frac{F_{ET}}{F_{WP}}.$$

It was also determined that the range of the rational displacement velocity of the ET is for each magnitude of the IEG, which provide a stable flow of the μECM process, due to the performance of the evacuation conditions of the products ($\xi \leq \xi_c$, $T < T_c$), as well as improving process productivity by the ET velocity increase.

Acknowledgements

The reported study was founded by RFBR and Tula region according to the research project №15-48-03250p_a.

References

[1] Davydov A.D., Kozak E. High-speed electrochemical shaping. Science. Moscow. 1990.
[2] Davydov A.D., Volgin V.M., Lyubimov V.V. Electrochemical machining of metals: Fundamentals of Electrochemical Shaping. Russian Journal of Electrochemistry, 2004. V.40. N 12. P.1230-1265.
[3] Lyubimov V.V. The investigation on improving the accuracy of electrochemical formation at small interelectrode gaps. Tula. 1973.
[4] Sedikin V.F. Environment for the dimensional electrochemical treatment machine parts. Mechanical Engineering, Moscow. 1980.
[5] Venevtsev A.U. Microelectrochemical machining with ultra-small interelectrode gap and applying microsecond voltage pulse. Tula State University. Tula. 2014.
[6] Volgin V.M., Lyubimov V.V., Kukhar V.D., Davydov A.D. Modeling of wire electrochemical micromachining. Procedia CIRP. 2015. V.37. P.176-181.
[7] Volgin V.M., Lyubimov V.V., Davydov A.D. Modeling of numerically controlled electrochemical micromachining. Chemical Engineering Science. 2016. V.140. P.252-260.
[8] Volosatov V.A. Handbook of electrochemical and electrical treatment methods. Mechanical Engineering, Moscow. 1988.